2000

Diffusion of Water in Nafion 115 Membranes

Sathya Motupally

Aaron J. Becker

John W. Weidner
University of South Carolina - Columbia, weidner@engr.sc.edu

Publication Info

Journal of the Electrochemical Society, 2000, pages 3171-3177.

Publisher's link: http://dx.doi.org/10.1149/1.1393879
DOI: 10.1149/1.1393879

Journal of The Electrochemical Society, **147** (9) 3171-3177 (2000)
S0013-4651(99)12-082-2 CCC: $7.00 © The Electrochemical Society, Inc.

Diffusion of Water in Nafion 115 Membranes

Sathya Motupally,[a,*] Aaron J. Becker,[b,*] and John W. Weidner[a,*,z]

[a]*Center for Electrochemical Engineering, Department of Chemical Engineering, University of South Carolina, Columbia, South Carolina 29208, USA*
[b]*E. I. DuPont de Nemours and Company, Central Research and Development, Wilmington, Delaware 19880-0323, USA*

In this paper, experimental and simulated data for the diffusion of water across Nafion membranes as a function of the water activity gradient are presented. The gradient in the activity of water across the membrane was varied by changing the flow rate and pressure of nitrogen gas on one side of the membrane. The other side of the membrane was equilibrated with liquid water. It was found that the model predictions are very sensitive to the value of the diffusion coefficient of water in Nafion. Using the Fickian diffusion coefficient extracted from self-diffusion measurements reported in the literature, the model simulations matched experimental data with less than 5% error over a wide range of operating conditions.

Manuscript submitted December 23, 1999; revised manuscript received April 26, 2000.

In the past decade, interest and investment in the research and development of hydrogen/oxygen fuel cells based on polymeric electrolytes has increased. The most commonly used polymeric membrane in fuel cells is Nafion (DuPont), which functions as the separator and also as the electrolyte for proton transport.[1-12] Nafion membranes can conduct protons only in the presence of water, and proton conductivity decreases with a decrease in the level of hydration of the membrane.[1-12] Therefore, under most operating conditions, to keep the membrane hydrated on both sides, humidified hydrogen and oxygen (or air) are fed to the anode and the cathode of the fuel cell, respectively. Under a load, hydrogen is oxidized to protons at the anode and these protons are transported to the cathode through the ionomer dispersed in the catalyst layer and the polymer electrolyte membrane. At the cathode, oxygen is reduced to water by these protons. The production of water at the cathode results in a gradient in the activity of water across the Nafion membrane. This gradient results in the diffusion of water from the cathode to the anode. Water is also transported from the anode to the cathode along with the protons. This phenomenon is called the electro-osmotic drag of water. The net water flux across the membrane under any operating condition is a combination of diffusion and electro-osmotic drag.[1-7] Managing the transport of water across the membrane is critical for the proper operation of a fuel cell.

Mathematical models of polymer electrolyte membrane fuel cells (PEMFCs) are effective research and development tools. A number of reports on modeling PEMFCs have been published in the literature.[1-6] The performance index of PEMFCs is the deliverable power density, and the goal of PEMFC models is to reliably predict the cell voltage *vs*. applied current under a variety of operating conditions. Losses in power density during the operation of a PEMFC accrue from activation, ohmic, and mass transport overpotentials at the anode and the cathode. For the calculation of these overpotentials, an accurate description of the net flux of water across the membrane is essential. For example, the level of hydration of the membrane, which governs the conductivity and therefore the ohmic overpotential, depends on the net amount of water transported across the membrane. The calculation of the net water transport across the membrane requires an accurate description of the diffusion flux and the flux due to electro-osmotic drag.

The objective of this paper is to quantify the diffusion flux of water across Nafion 115 membranes. In order to accomplish this objective, information is needed on the diffusion coefficient of water as a function of the water content of the membrane and the equilibrium relationship between the activity of water in the gas phase and the water content of the membrane. The water content of the membrane, λ, is defined as the number of moles of water associated with a mole of the sulfonic acid groups in Nafion. The water content of Nafion membranes has been measured by Hinatsu *et al*.,[8] Escoubes and Pineri,[9] and Zawodzinski *et al*.[10-12] and the results reported by the three groups are similar.

Unfortunately, three different values of the diffusion coefficient of water through Nafion have been reported in the literature. First, using nuclear magnetic resonance (NMR) techniques, Zawodzinski *et al*.,[11] measured the diffusion coefficient of $_1$H as a function of the water content of the membrane. Arguing that the movement of $_1$H need not necessarily represent the diffusion of water, Fuller[5] measured the Fickian diffusion coefficient of water by measuring the flux across Nafion membranes equilibrated with water on one side and flowing nitrogen gas on the other. Their experimental setup, however, made it difficult to predict the activity of water at the surface of the membrane in contact with the gas. Nguyen and White[3] derived an expression for the Fickian diffusion coefficient of water in Nafion based on fuel cell performance data in the literature and the electro-osmotic drag measurements of Springer *et al*.[1]

In this paper, we compare water flux calculations across Nafion 115 membranes with experimental water flux measurements. The water flux calculations were carried out using the three diffusion coefficients reported.[3,5,11] Experimentally, the flux of water across Nafion was measured as a function of the nitrogen gas flow rate, at 80°C and 1.0 and 5.0 atm pressure, in a fuel cell setup. It was found that the flux of water could be predicted accurately using the self-diffusion coefficient expression obtained for water using NMR techniques.[11] For the experimental conditions used in this work, we also simulate the water activity profiles in the flow channel and the water content profiles across the membrane, to gain further insight into the transport of water across the Nafion membrane.

Experimental

The water flux measurements were carried out in a fuel cell comprised of Kynar/graphite composite plates, stainless steel end plates, and copper current collectors. Both sides of the cell contained E-TEK carbon cloth diffusion backings and flow channels machined into the carbon current collectors. The flow channel was a single serpentine channel with a depth and width of 0.076 and 0.16 cm, respectively. The thickness of the diffusion backing was 250 μm with a porosity of approximately 60%. A Nafion 115 membrane with catalyst layers coated on both sides was inserted between the gas diffusion backings, and the cell was assembled by the application of a uniform pressure of 5 psi between the copper plates on either side. The catalyst layers contained 50/50 wt % Nafion 1100 ionomer and catalyst. The thickness of the catalyst layer on each side was approximately 10 μm, and the active area of the membrane was 50 cm^2.

A heating jacket was placed around the carbon current collectors, and the temperature was controlled at 80°C with the aid of thermocouples and automated temperature controllers. Water preheated to

* Electrochemical Society Active Member.
z E-mail: weidner@engr.sc.edu

S0013-4651(99)12-082-2 CCC: $7.00

80°C was circulated through one side of the fuel cell and nitrogen passed through the other side. The measured water flux data were independent of the temperature of the inlet nitrogen stream. For experimental simplicity, unheated nitrogen was passed through the gas side. Water was delivered with the aid of a piston pump, and the pumping rate was fixed so as to deliver 150 cm^3/min of water. The flow rate of nitrogen was controlled by a Brooks mass flow controller. The flow range of the controller was 30-4000 cm^3/min at standard temperature and pressure (STP). The pressure of each side of the cell was controlled with back-pressure regulators and recorded with pressure gauges on the outlet and inlet of either side of the membrane. All experiments were conducted under conditions at which the pressure on both the sides of the membrane was approximately the same.

The nitrogen gas fed to the cell was dry. As the gas traversed the length of the cell, its humidity increased due to the diffusion of water across the Nafion membrane. To measure the amount of water diffusion across the membrane, the nitrogen exiting the cell was passed through a vertical polyvinyl chloride (PVC) knock-out vessel maintained at 20°C. The amount of water exiting the cell is the sum of the water collected in the knock-out vessel plus the amount of water vapor leaving the knock-out vessel with the nitrogen stream. The molar flow rate of water in this cooled gas stream is equal to the saturated mole fraction of water at 20°C multiplied by the total molar flow rate of gas and vapor. For example, at 1.0 atm and at a molar flow rate of 2.97×10^{-3} mol/s of nitrogen (4000 cm^3/min, STP), the molar flow rate of associated water vapor is 5.0×10^{-5} mol/s. This is equal to a mass flow rate of 0.05 g/min and is approximately 9.0% of the total water exiting the cell.

The knock-out vessel was equipped with a piezoelectric level sensor. Condensation of water in the vessel results in a decrease in the resonant frequency of the alternating signal emanating from the sensor, which in turn correlates to a mass increase. This frequency decrease relative to the frequency of a reference crystal in air was used to calculate the mass of the water condensed. This mass was monitored continuously, and the rate of water condensing was calculated from the slope of a straight-line fit through the data (see Fig. 3 for representative data). The flux data presented in this paper are an average of three sets of experiments. Error bars indicating the maximum and minimum values are provided with the experimental data.

Model Development

The activity of water at the surface of the Nafion membrane was controlled by varying the flow rate of nitrogen. This, however, results in a nonuniform activity of water in the channel because water accumulates in the gas phase as the nitrogen passes through the channel. It is, therefore, necessary to develop a model to predict the activity of water as a function of position in the flow channel. A schematic of the side view of the cell is shown in Fig. 1a, and a three-dimensional view of the flow channel on the gas side is shown in Fig. 1b. As seen in Fig. 1a and b, the serpentine flow configuration on the gas side is represented as a single parallel channel with a width, depth, and length of w_1, d, and L, respectively. The width and thickness of the catalyst-coated Nafion membrane are denoted w_2 and δ_M, respectively. The assumptions used in the development of the model are given below:

Assumptions:

1. The Nafion membrane is the dominant resistance to the transport of water. Therefore, the concentration of water is uniform across the gas diffusion cloth and the flow channel.
2. Diffusion of nitrogen across the membrane is negligible.
3. The nitrogen/water vapor mixture in the flow channel obeys the ideal gas law.
4. The two interfaces of the membrane are in equilibrium with the flow channel.
5. The thickness of the hydrated and the dry catalyst-coated Nafion membranes are equal.
6. The entire fuel cell system is maintained at a uniform and constant temperature throughout.
7. The permeability of water across the Nafion membrane is negligible.[2]

Assumption 1 is valid because the diffusion coefficient of water vapor in nitrogen is at least four orders of magnitude greater than the diffusion coefficient of water in Nafion, and the diffusion lengths are comparable. The validity of assumption 2 is based on the work by Broka *et al*.,[13] who showed that the flux of hydrogen across Nafion is negligible. The ideal gas law is valid at the pressures and temperatures employed here (*i.e.*, assumption 3). The water flux data are recorded at steady state, allowing the membrane surfaces to equilibrate (*i.e.*, assumption 4). It has been shown that during equilibration with water, Nafion membranes swell. The thickness of hydrated Nafion membranes increases linearly with an increase in λ.[1] For measurements on freely suspended Nafion membranes,[5,11] it is necessary to consider the variation in the thickness with the level of hydration. However, in our case, wherein the membrane is held tightly under pressure between graphite plates, it is assumed that the thickness of the membrane is invariant with the level of hydration (*i.e.*, assumption 5). A uniform and constant temperature (*i.e.*, assumption 6) was assured by placing a heating jacket around the carbon current collectors. The water flowing through one side of the cell was also maintained at the same temperature as that of the cell. Although the nitrogen did not enter at this temperature, the data reported here were independent of nitrogen's inlet temperature. Finally, considering the fact that all experiments during this work were performed with approximately the same pressure on the water and

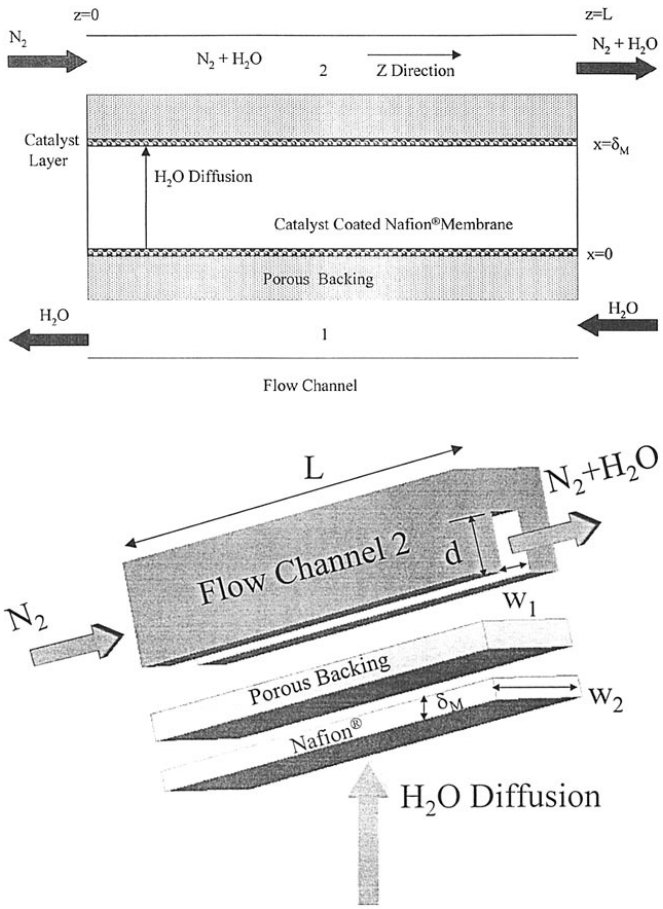

Figure 1. (a, top) Schematic of the side view of the experimental cell. Dry nitrogen and water are fed to flow channels 2 and 1, respectively. Water diffuses across the Nafion membrane from the liquid to the gas side due to a gradient in the activity of water. (b, bottom) Schematic of a three-dimensional view of the single parallel channel representation. The width, depth, and length of the channels are denoted w_1, d, and L, respectively. The width of the catalyst-coated membranes is denoted w_2.

S0013-4651(99)12-082-2 CCC: $7.00

gas sides, combined with the low permeability values of Nafion,[2] the permeability of water across the membrane is negligible (*i.e.*, assumption 7).

Material balance for water vapor in the flow channel.—Due to the diffusion of water across the membrane, the mole fraction of water vapor in the nitrogen stream increases as the gas traverses through the cell. The change in the number of moles of water vapor in the flow channel is proportional to the local flux of water into the flow channel from across the membrane. The differential mole balance for water in the flow channel can be represented mathematically as

$$\frac{dN_{w,z}}{dz} - \left(\frac{w_2}{w_1 d}\right) N_{w,x} = 0 \qquad [1]$$

The axial flux of water at any point in the flow channel is related to the mole fraction of water vapor in the gas phase by

$$N_{w,z} = N^0_{N_2}\left(\frac{y_w}{1 - y_w}\right) \qquad [2]$$

In Eq. 2, $N^0_{N_2}$ is the flux of nitrogen entering the flow channel. Due to assumption 2, this flux is constant throughout. Substituting Eq. 2 into Eq. 1 gives

$$\frac{N^0_{N_2}}{(1 - y_w)^2}\frac{dy_w}{dz} - \left(\frac{w_2}{w_1 d}\right) N_{w,x} = 0 \qquad [3]$$

Integrating Eq. 3 over the length of the flow channel and substituting the value for y_w at $z = L$ into Eq. 2 gives the total flux of water crossing the membrane. Performing this integration requires an expression for $N_{w,z}$ as a function of y_w.

Material balance for liquid water across the membrane.—At steady state, the flux of water across the membrane in the x direction is a constant. The flux of water across the membrane can, however, vary in the z direction (see Fig. 1a or b). Therefore

$$\frac{dN_{w,x}}{dx} = 0 \qquad [4]$$

The flux of water is proportional to the gradient in the water content of the membrane and can be represented by Fick's law as

$$N_{w,x} = -\frac{\rho_M}{M_M} D_{w,F}\frac{d\lambda}{dx} \qquad [5]$$

where $D_{w,F}$ is the Fickian diffusion coefficient of water in the membrane and $(\lambda\rho_M/M_M)$ is the concentration of water in the Nafion membrane. Because $N_{w,x}$ is constant, Eq. 4 can be integrated from x equal to 0 to δ_M to give

$$N_{w,x}(z) = -\frac{\rho_M}{M_M\,\delta_M}\int_{\lambda_1}^{\lambda_2} D_{w,F}\,d\lambda \qquad [6]$$

The lower and upper limits of integration in Eq. 6 represent the water content of the membrane on the water and nitrogen sides, respectively.

Zawodzinski *et al*.[10] measured the water content of a Nafion 117 membrane in contact with water vapor, and they reported the following relationship between λ and the activity of water

$$\lambda = 0.043 + 17.81a_w - 39.85a_w^2 + 36.0a_w^3 \qquad [7]$$

where the activity of water in the vapor phase is given by

$$a_w = \frac{y_w P}{P^*(T)} \qquad [8]$$

and the vapor pressure of water as a function of temperature, $P^*(T)$, is given by[1]

$$\log[P^*(T)] = -2.18 + 0.029(T - 273.2) - 9.18 \times 10^{-5}(T - 273.2)^2 + 1.44 \times 10^{-7}(T - 273.2)^3 \qquad [9]$$

where T is in kelvin. Although Eq. 7 was obtained using measurements at 30°C, it is assumed to hold at other temperatures.[1,3] According to Eq. 7, the water content of the membrane increases from 0.043 to 14.0 as a_w in the vapor phase increases from zero to unity. However, when Nafion membranes are equilibrated with liquid water at 80°C (*i.e.*, $a_w = 1.0$), a λ value of approximately 17 was measured.[1,3,6] The difference in the water uptake characteristics of polymeric membranes from vapor and liquid phases of identical activities is termed the "Schroeders paradox."[14] In this work, we assume that λ instantaneously increases from 14 to 17 on the nitrogen side as water condenses.

The remaining parameter needed to calculate the flux of water across the membrane is the Fickian diffusion coefficient of water, $D_{w,F}$, as a function of λ. Zawodzinski *et al*.[11] measured the intra- or self-diffusion coefficient of water, $D_{w,I}$, at 30°C using pulsed gradient nuclear magnetic resonance spectroscopy. They reported six values of $D_{w,I}$ ranging from 0.80×10^{-6} to 7.2×10^{-6} cm^2/s as λ increased from 2 to 22. Note that at λ value of 22 is attained when the membrane is equilibrated with liquid water at 30°C, compared to a value of 17 when equilibrated with liquid water at 80°C. We fit these six values of $D_{w,I}$ to an empirical expression and obtained

$$D_{w,I} = 6.31 \times 10^{-7}(\lambda - 0.0209 \quad \lambda^2 - 0.501) \qquad [10]$$

For systems where the transport number of electrons is zero or unity, the intra- and Fickian diffusion coefficients are related through the "Darken factor" given below[16]

$$D_{w,F} = D_{w,I}\underbrace{\left[\frac{\partial \ln(a_w)}{\partial \ln(\lambda)}\right]}_{\text{Darken factor}} \qquad [11]$$

The Darken factor was obtained by taking the reciprocal of the differential of the Eq. 7 with respect to a_w. This results in an expression for the Darken factor in terms of a_w. Division of Eq. 10 by the Darken factor obtained using the formula shown in Eq. 11 yields the expression for the Fickian diffusion coefficient. However, because this expression for the Fickian diffusion coefficient was obtained from self-diffusion coefficient data and the water uptake isotherm measured at 30°C, its validity is limited to only that temperature. Therefore to account for temperature differences, we corrected the resulting Fickian diffusion coefficient data with the enthalpy of diffusion of 4.84 kcal/(mol K) as measured by Yeo and Eisenberg.[15] Equation 12 given below is the final form of the Fickian diffusion coefficient as a function of water content and temperature

$$D_{w,F} = 3.10 \times 10^{-3}\,\lambda(-1 + e^{0.28\lambda})\,\exp\left[\frac{-2436}{T}\right] \quad (\text{for } 0 < \lambda \le 3) \qquad [12a]$$

$$D_{w,F} = 4.17 \times 10^{-4}\,(1 + 161e^{-\lambda})\,\exp\left[\frac{-2436}{T}\right] \quad (\text{for } 3 \le \lambda < 17) \qquad [12b]$$

The discontinuity in Eq. 12 results from the functional dependence of the Darken factor (Eq. 11) in terms of λ. The discontinuity prevents a single equation from accurately describing the diffusion coefficient over the complete range of λ.

The diffusion coefficient expression given by Fuller[5] can be simplified and represented as a function of λ and temperature as given below

$$D_{w,F} = 2.1 \times 10^{-3}\lambda\,\exp\left[\frac{-2436}{T}\right] \qquad [13]$$

Nguyen and White[3] report the Fickian diffusion coefficient in terms of the activity of water. Using Eq. 7, their expression can be converted to a function of λ to given

$$D_{w,F} = (1.76 \times 10^{-5} + 1.94 \times 10^{-4}\lambda)\,\exp\left[\frac{-2436}{T}\right] \qquad [14]$$

S0013-4651(99)12-082-2 CCC: $7.00

A plot of the Fickian diffusion coefficient of water reported by Zawodzinski *et al.*[11] (Eq. 12), Fuller[5] (Eq. 13), and Nguyen and White[3] (Eq. 14) as a function of λ at 80°C is shown in Fig. 2. Equations 13 and 14 are linearly dependent on the water content of the membrane, whereas Eq. 12 shows a maximum at $\lambda = 3.0$.

Solution procedure.—Substituting the Fickian diffusion coefficient of water (Eq. 12, 13, or 14 into Eq. 6 and integrating gives an analytical solution to the flux of water across the membrane as a function of λ_1 and λ_2. The value of λ on the water side of the membrane (*i.e.*, λ_1) is fixed at 17.0, and λ on the nitrogen side (*i.e.*, λ_2) varies depending upon the mole fraction of water in the vapor phase. therefore, $N_{w,x}$ is a function only of y_w, and Eq. 3 can be integrated to give y_w at each point in the flow channel. The integration was performed using a fourth-order runge-kutta routine with a fixed step size of 0.0001. The total flux of water crossing the membrane is obtained by evaluating y_w at the channel exit (*i.e.*, $z = L$), and substituting this value into Eq. 2.

Results and Discussion

At various volumetric flow rates of nitrogen, the mass of water condensing in the knock-out vessel was recorded at regular intervals. The data were collected at a cell temperature of 80°C and pressures of 1.0 and 5.0 atm. Figure 3 displays mass *vs*. time data at representative volumetric flow rates of nitrogen at the temperature and pressure conditions of the cell. Linearly regressed fits to the data are also shown in Fig. 3. The total flux of water diffusing across the membrane is related to the rate at which liquid water is collected in the knock-out vessel plus the rate at which water vapor is leaving with the nitrogen stream exiting the knock-out vessel, which is maintained at 20°C. The first quantity, which represents over 90% of the total water, is obtained by dividing the slope of the data in Fig. 3 by the molecular weight of water (18 g/mol) and the area of the membrane (50 cm^2). The second quantity, the rate at which water associated with the nitrogen stream leaves the knock-out vessel, is calculated from the right side of Eq. 2 by substituting y_w equal to $P^*(20°C)/P$.

It can be seen from Fig. 3 that the slope of the lines, and therefore the total flux of water diffusing across the membrane, increases with an increase in the volumetric flow rate of nitrogen. For example, at 1.0 atm, the flux of water increases from 0.13 to 0.35 g/min as the flow rate of nitrogen increases from 300 to 800 cm^3/min. At higher flow rates of nitrogen (3000 and 4000 cm^2/min), the flux of water is constant and equal to 0.49 g/min. Also, at a particular flow rate of nitrogen, the flux of water across the membrane is lower at a higher pressure. For example, at 800 cm^3/min, the slopes at 1.0 and 5.0 atm are 0.35 and 0.22 g/min, respectively. It is important to note that the molar flow rate of nitrogen through the cell at a volumetric flow rate of 800 cm^3/min and 5.0 atm is the same as that in the case of 4000 cm^3/min and 1.0 atm.

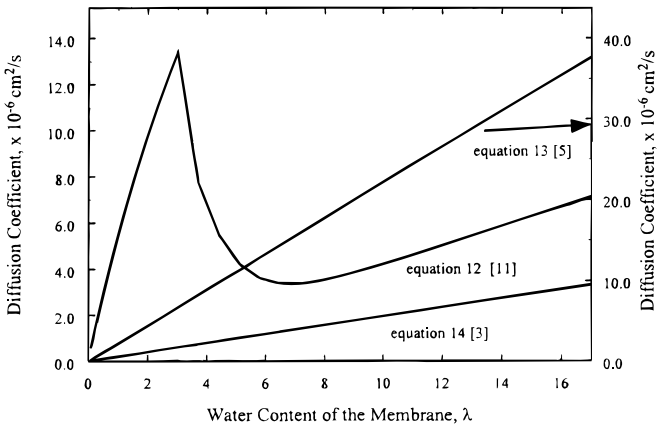

Figure 2. Fickian diffusion coefficient values reported by Fuller (Eq. 13),[5] Nguyen and White (Eq. 14),[3] and Zawodzinski *et al*. (Eq. 12)[11] at a temperature of 80°C. Equations 13 and 14 are linearly dependent on the water content of the membrane. Equation 12 shows a maximum at $\lambda = 3$ due to the nature of the equilibrium relationship as given by 7.

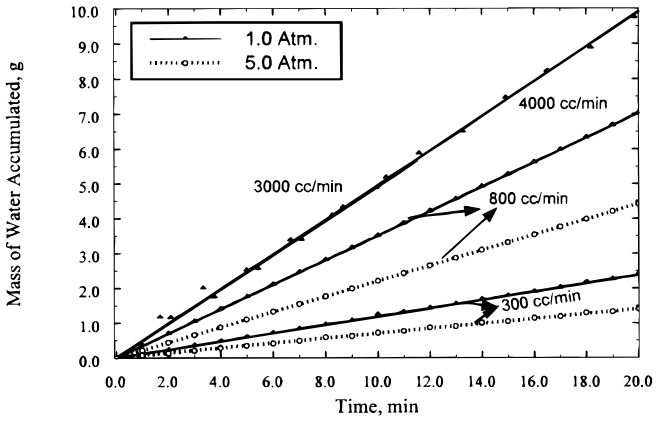

Figure 3. Plot of mass of water accumulated in the knock-out vessel *vs*. time. Symbols represent experimental data, and the lines indicate regressed linear fits. The slopes of the regressed fits were used to calculate the flux of water. The straight-line behavior is indicative of a steady-state process.

The trends seen in Fig. 3 can be explained by considering the activity of water in the nitrogen stream. Water diffuses across the Nafion membrane from the liquid side to the gas side due to a gradient in the activity of water. The activity of water on the liquid side is unity, and the activity of water in the gas phase varies in the axial direction (*i.e.*, along *z*) in the flow channel. At the cell entrance ($z = 0$), the activity of water is zero resulting in a maximum in the gradient. As the gas traverses the channel, water vapor accumulates in the flow channel resulting in a decrease in the local flux of water with increasing *z*. Finally, after sufficient accumulation of water in the channel, the activity of water reaches unity thereby resulting in the condensation of water. Consequently, liquid water of the same activity is present on both sides of the membrane and diffusion of water ceases.

Therefore, the local flux of water across the membrane is a maximum at the channel inlet, decreases with an increase in *z* until it vanishes at the point of condensation. The total flux is a sum of the local flux at every point in the *z* direction. At a constant temperature, an increase in the volumetric flow rate of nitrogen or a decrease in the cell pressure results in an increase in the total flux of water across the membrane. This is due to a decrease in the activity of water in equilibrium with the membrane on the gas side. The effect of the variation of the flow rate and pressure on the diffusion flux of water can be easily seen from Eq. 15 given below. Equation 15 was obtained by solving for y_w from Eq. 2, substituting the resulting expression into Eq. 8, and converting from a molar to a volumetric flow rate using the ideal gas law

$$a_w = \frac{\dot{V}_w}{\dot{V}_w + \dot{V}^o_{N_2}} \frac{P}{P^*(T)} \qquad [15]$$

Equation 15 indicates that a decrease in the cell pressure results in a decrease in the water activity at each axial position in the channel. This results in an increase in the water activity gradient throughout, and consequently an increase in the total flux of water crossing the membrane. Similarly, an increase in the nitrogen flow rate decreases the water activity. At very high flow rates, the denominator in Eq. 15 tends to infinity resulting in a zero activity of water throughout. Under such conditions, a maximum diffusion flux of water that is insensitive to the flow rate of nitrogen is obtained.

The total flux of water as a function of the volumetric flow rate of nitrogen and cell pressure is summarized in Fig. 4. The experimental data in Fig. 4 are represented by symbols (open and closed symbols correspond to 5.0 and 1.0 atm, respectively). The solid curves correspond to 1.0 atm and result from the solution to Eq. 6

S0013-4651(99)12-082-2 CCC: $7.00

coupled with Eq. 12, 13, or 14. The dashed curve corresponds to 5.0 atm, and only the solution to Eq. 6 coupled with Eq. 12 is shown. The input parameters required for the simulations were either measured or taken from the literature (see Table I for details).

Figure 4 illustrates the effect of the choice of the diffusion coefficient on calculated water flux. It is clear that good agreement between the experimental and calculated data is possible only with the use of Eq. 12 for the Fickian diffusion coefficient of water. Calculations using Eq. 12 match experimental data with less than 5% error for all flow rates and pressures. Use of Eq. 13 and 14 results in the over and under prediction of the water flux by factors of 4.5 and 3.5, respectively, at higher flow rates. From the data shown in Fig. 4, it can be concluded that the Fickian diffusion coefficient extracted from the self-diffusion measurements accurately describes diffusion across the Nafion membrane. However, in most polymer electrolyte membrane (PEM) fuel cell performance models the validity of self-diffusion coefficient measurements is usually discounted.[3,5,6] This contention stems mainly from the fact that the diffusion coefficient measured is for ^{1}H and nuclear magnetic resonance (NMR) measurement do not differentiate between the ^{1}H contained in water *vs*. the protons associated with the sulfonic acid side chains. Therefore, the measured diffusion coefficient is representative of an average proton environment in the membrane, and attributing the measured values at different water contents to the diffusion coefficient of water could be erroneous. However, as stated by Zawodzinski *et al*.,[11] the NMR measurements are valid for higher water contents where the ^{1}H content in the membrane water is much larger than that associated with the sulfonic acid side chains. Also, the protons and the water diffuse at approximately the same rate due to vehicular diffusion (Grotthus-Hopping) mechanism. However, at lower water contents, the diffusion coefficient of water measured by NMR could actually be underpredicted due to the relative immobility of the protons.

The results of this work show that the findings of the NMR diffusion work[11] are also valid at lower water contents of the membrane. This is true because the model using Eq. 12 can accurately predict water flux with no adjustable parameters, even at flow rates for which the average activity of water in equilibrium with the membrane is less than 0.5. For example, at a flow rate of 3000 cm^3/min, the average activity of water is less than 0.5 and no water condenses in the flow channel.

Even though we can fit the water flux data reported in this paper by manipulating Eq. 13 or 14, doing so should be strongly dissuaded. This is primarily because, even though the overall flux may be predicted with a particular diffusion coefficient function, it does not necessarily mean that the calculated water content profiles in the membrane will be accurate. Accurate prediction of the water content of the membrane is very important for predicting the electrochemical performance of the Nafion membranes in fuel cells. Therefore, to accurately predict the water content profiles along with the overall water flux, it is necessary to use the diffusion coefficient given in Eq. 12.

Table I. Parameters used in the simulations.

		Reference
Area of membrane (A)	50.0 cm^2	a
Channel width (w_1)	0.159 cm	a
Channel depth (d)	0.076 cm	a
Effective membrane width (w_2)	0.36 cm	b
Length of channel (L)	136 cm	a
Molecular weight of membrane (M_M)	1100 g/mol	1
Thickness of membrane (δ_M)	0.015 cm	a
Vapor pressure of Water (P^*)	0.461 atm	1
Water content (λ)	Eq. 7	
Diffusion coefficient of water ($D_{w,F}$)	Eq. 12, 13, or 14	11, 5, or 3
Total pressure (P)	1.0 or 5.0 atm	a
Density of membrane (ρ_M)	2.0 gm/cm^3	11

[a] Indicates measured values.
[b] w_2 is calculated by dividing the membrane area (A) with the effective length of the serpentine flow channel (L).

In order to gain additional insight into the water management issues in PEM fuel cells the total water flux data and corresponding simulation at 1.0 atm cell pressure from Fig. 4 are replotted in Fig. 5 on a linear scale. To show the effect of the temperature of the inlet nitrogen gas on the flux of water, data at 1.0 atm for the case wherein nitrogen was preheated to 80°C are also shown. The dotted curve represents simulations obtained by using Eq. 16 to relate a_w to λ, rather than Eq. 7. Equation 16 is the water-uptake isotherm reported by Hinatsu *et al*.,[8] measured at 80°C

$$\lambda = 0.3 + 10.8a_w - 16.0a_w^2 + 14.1a_w^3 \qquad [16]$$

First, it can be seen from Fig. 5 that the effect of the temperature of the nitrogen gas fed to the cell is negligible. The water crossover rate for nitrogen fed at 80°C falls within the error bars for the three data sets collected for the room-temperature feed. The water flux is independent of the inlet feed temperature because the time constant

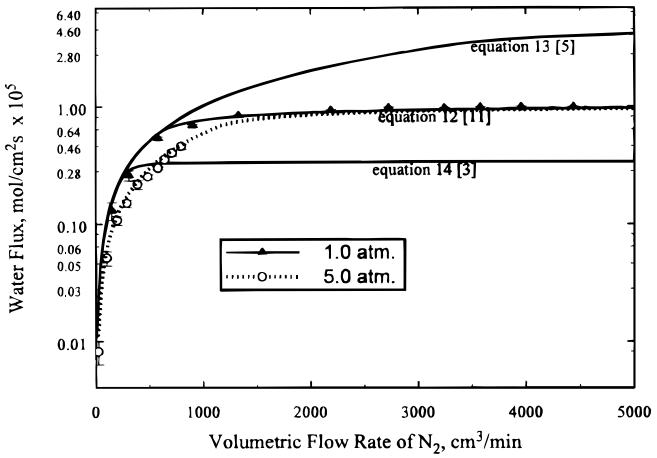

Figure 4. Simulated and experimental water flux data as a function of the volumetric flow rate of nitrogen at 80°C. The symbols represent experimental data, and the curves represent model simulations. Use of Eq. 12 for the Fickian diffusion coefficient of water results in an accurate prediction of the flux of water across the membrane. Calculations based using Eq. 13 and 14 over and under predict the flux of water, respectively.

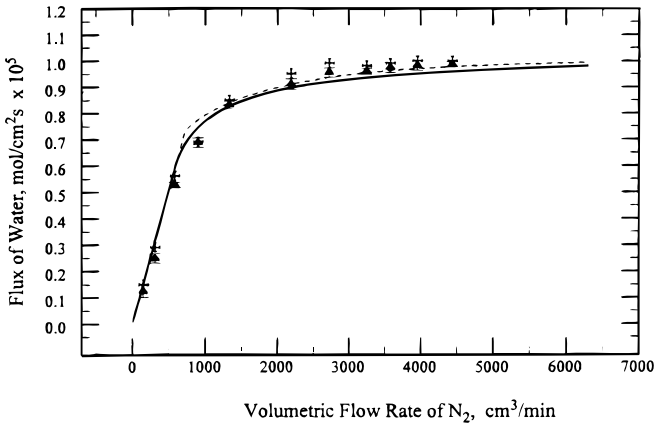

Figure 5. Water flux data at 1.0 atm cell pressure as a function of volumetric flow rate of nitrogen at 80°C. The symbols represent data for the cases where the inlet nitrogen temperature is 80 and 30°C (✠ = 80°C, ▲ = 30°C). The solid curve represents model simulation using Eq. 7, and the dotted curve represents simulations using Eq. 16. There is negligible effect of inlet nitrogen temperature on the water flux across the membrane. Also, there is less than 4% error in the model predictions using Eq. 7 and 16.

S0013-4651(99)12-082-2 CCC: $7.00

for heat conduction through the nitrogen from the channel walls ($4C_p\rho d^2/\kappa \approx 0.005$ s) is orders of magnitude smaller than the time constant for convection, even at the highest flow rate ($L/v > 150$ s). (Note: C_p, ρ, κ are the specific heat capacity, molar density, and thermal conductivity of nitrogen gas. Also, v is the superficial velocity of the nitrogen gas in the flow channel.) Therefore, the nitrogen feed reaches the temperature of the system almost instantaneously upon entering the flow channel. No temperature gradients exist for the vast majority of the channel length.

Second, it can be seen by comparing the dotted and solid curves that there is very little difference between water flux calculations obtained by using Eq. 7 or 16. In fact the maximum difference between the result between the simulations using Eq. 7 and Eq. 16 is approximately 4%. This is primarily because Eq. 7 and 16 are quantitatively similar at lower water activities ($a_w < 0.7$). For $a_w > 0.7$, the water content of the membrane calculated using Eq. 7 is greater than those obtained via Eq. 16. However, due to the relatively smaller driving force (*i.e.*, water content gradient) across the membrane at higher a_w values, there is a negligible effect on the simulations.

As can be seen from the figure, the flux of water increases linearly with the volumetric flow rate of nitrogen and gradually asymptotes to a constant value at higher flow rates. For example, at 1.0 atm, the flux of water increases linearly from $1. \times 10^{-6}$ to 5.0×10^{-6} mol/cm^2-s as the flow rate of nitrogen increases from 100 to 600 cm^3/min. For flow rates in the 700-2000 cm^3/min range, the flux of water varies in a nonlinear manner and is a constant and equal to 9.9×10^{-6} mol/cm^2-s for flow rates greater than 2000 cm^3/min. Similar trends are also observed for the 5.0 atm data. However, as mentioned earlier, due to the higher activity of water in the flow channel at the higher pressure, the corresponding water flux is lower. It can also be seen from Fig. 5 that irrespective of the cell pressure, the flux of water asymptotes to the same limiting value at high flow rates. Unfortunately, this aspect cannot be seen in the 5.0 atm experimental data because of the limit of the maximum flow output of the mass flow controllers. At 5.0 atm cell pressure, the maximum flow rate range of the mass flow controller used was only 800 cm^3/min.

The water flux calculations shown in Fig. 4 and 5 require the calculation of the water activity profiles in the flow channel. Figure 6 shows selected water activity profiles in the flow channel, and insight into the qualitative trends seen in Fig. 5 can be obtained from the water activity profiles. Under all conditions, due to the use of dry nitrogen, the activity of water vapor at the inlet of the flow channel is zero. As seen from the figure the activity of water increases with an increase in z due to the diffusion of water across the Nafion membrane. Water crossover is arrested when the partial pressure of water equals the ratio of the saturated vapor pressure to the cell pressure. At this stage, the activity of water vapor is equal to unity and the quality of the gas stream is invariant with a further increase in z.

As can be seen from Fig. 6, condensation of water occurs at lower flow rates and higher pressures. Lower flow rates and higher cell pressures result in a rapid increase in the partial pressure of water with values reaching the saturated vapor pressure before the gas mixture reaches the exit of the flow channel. For example, as shown in Fig. 6, at nitrogen flow rates of 200 and 600 cm^3/min and 1.0 atm cell pressure, the nitrogen gas traverses 25 and 95% of the length of the flow channel prior to condensation (*i.e.*, $z/L = 0.25$ and 0.95), respectively. At 1.0 atm, with an increase in the flow rate of nitrogen from 600 to 1000 cm^3/min, condensation of water is eliminated. According to Eq. 2, the linear relationship between water flux and nitrogen flow rate is possible only under conditions wherein the mole fraction of water at the exit of the gas flow channel is a constant. As can be seen from Fig. 5 and 6, the linear relationship between the water flux and nitrogen flow rate is due to condensation. Due to condensation, the mole fraction at the exit of the flow channel is a constant and equal to $P^*(T)/P$, and therefore the flux of water varies linearly with the flow rate.

At 1.0 atm, with an increase in the flow rate of nitrogen above 600 cm^3/min, condensation is eliminated and the mole fraction of water vapor at the exit of the flow channel decreases with an increase in nitrogen flow rate. This results in the departure from the linear relationship between the overall water flux and nitrogen flow rate. With a further increase in the flow rate (>2000 cm^3/min), the activity of water tends to zero and the overall flux of water is invariant with flow rate. For example, at 4000 and 12000 cm^3/min, the average activities in the flow channel are 0.22 and 0.07, respectively. Even though the average activity of water decreases by a factor of three, the overall flux does not change appreciably due to the equilibrium relationship (Eq. 7) whereby the λ values in the $a_w = 0.1$-0.3 range are relatively constant. At 5.0 atm cell pressure, water condenses in the flow channel and all flow rates less than 1200 cm^3/min (not shown in Fig. 6). At 4000 and 12000 cm^3/min, the average values of a_w are approximately equal to those obtained for the 1.0 atm case. This results in limiting water flux data that is insensitive to cell pressure. This maximum water flux is a measure for the maximum water activity gradient that can be established across the membrane. At a constant temperature, this gradient is independent of the cell pressure.

The trends seen in Fig. 4 and 5 can be seen from the water activity profiles shown in Fig. 6. At any flow rate, as mentioned before, the total flux of water across the membrane is a sum of the local fluxes at all z. At every point in the z direction, due to the varying activity of water, the λ profiles across the membrane are also differ-

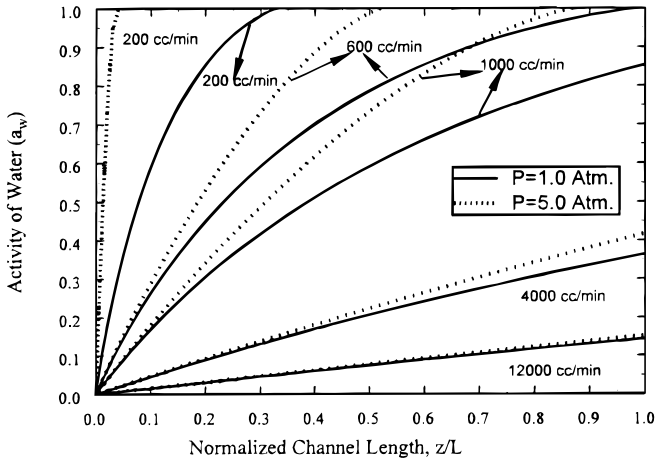

Figure 6. Simulated water activity *vs*. normalized channel length for 1.0 and 5.0 atm cell pressure and 80°C. The dashed curves represent simulations for 5.0 atm and the solid curves represent then 1.0 atm case. The activity of water decreases with an increase in the flow rate of nitrogen. When the activity of water reaches unity, water condenses in the flow channel.

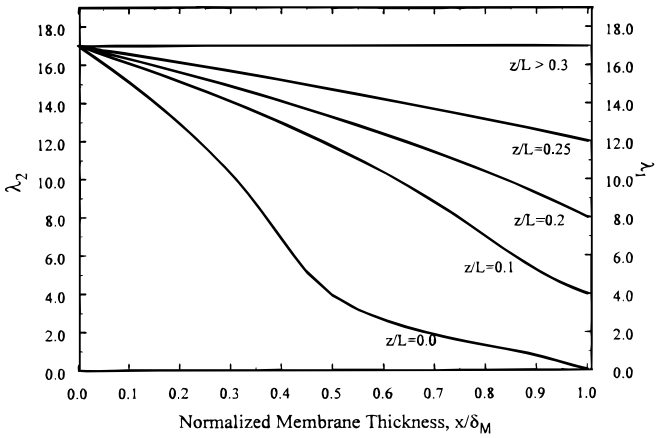

Figure 7. Water content profiles in the membrane as a function of normalized membrane thickness. The left abscissa corresponds to the water content at the membrane/liquid water interface (*i.e.*, λ_1) and right abscissa corresponds to the water content at the membrane/nitrogen interface (*i.e.*, λ_2).

S0013-4651(99)12-082-2 CCC: $7.00

ent. For example, λ profiles across the membrane for the 200 cm^3/min nitrogen flow rate and 1.0 atm cell pressure case are shown in Fig. 7. To obtain λ profiles across the membrane at different axial positions in the channel, the local activity of water calculated on the nitrogen side is converted to a local λ_2 value. This λ_2 value is used in Eq. 7, and the resulting expression solved for λ as a function of x. At $z = 0$, the nitrogen gas fed to the cell is dry and therefore the activity of water is equal to zero (*i.e.*, $\lambda_2 = 0.043$). Therefore, at the entrance of the cell the local water flux is the largest. As water accumulates in the nitrogen stream, the activity of water increases in the z direction. When z increases from 0 to 0.25, the activity of water increases from 0 to 0.8 and λ_2 increases from 0.043 to 12. As λ_2 increases, the local water flux decreases. For all z greater than 0.3, the activity of water is unity and therefore λ_2 is equal to 17. This leads to a zero gradient in λ across the membrane and results in the termination of diffusion. It can be seen from Fig. 7 that the membrane and results in the termination of diffusion. It can be seen from Fig. 7 that the λ profiles are not constant at any value of λ_2 (except 17, which represents zero flux conditions). A nonlinear λ gradient results in a constant flux of water across the membrane because the diffusion coefficient of water is a function of λ.

Conclusions

In this paper it is shown for the first time that the diffusion flux across a Nafion membrane can be accurately predicted by using the Fickian diffusion coefficient derived from self-diffusion measurements. Agreement to within 5% was obtained between model simulations and experimental diffusion flux data as a function of the activity gradient of water across the membrane. The activity gradient was varied by changing the flow rate of nitrogen and the cell pressure. An increase in the nitrogen flow rate increased the water activity gradient across the membrane and resulted in an increase in the diffusion flux. An increase in the cell pressure resulted in a decrease in the water activity gradient resulting in a decrease in the diffusion of water. This study can be used to improve the prediction of water management in PEM fuel cells.

Acknowledgments

The authors gratefully acknowledge the financial support from the Central Research and Development Division of E. I. DuPont. The authors also wish to thank D. Potter and T. Fleckenstein for help with the experiments.

The University of South Carolina assisted in meeting the publication costs of this article.

List of Symbols

a_w	activity of water
d	depth of the flow channel, cm
$D_{w,F}$	Fickian diffusion coefficient of water, cm^2/s
$D_{w,I}$	self-diffusion coefficient of water, cm^2/s
L	length of the flow channel, cm
M_M	molecular weight of membrane, cm
$N_{w,z}$	flux of water in the flow channel, mol/cm^2 s
$N_{w,x}$	flux of water across the membrane, mol/cm^2 s
$N^o_{N_2}$	flux of nitrogen at the inlet of the flow channel, mol/cm^2 s
P	pressure, atm
P^*	vapor pressure of water, atm
T	temperature, K
$\dot{V}_w$	volumetric flow rate of water vapor, cm^3/min
$V^o_{N_2}$	volumetric flow rate of nitrogen at the inlet of the flow channel, cm^3/min
w_2	width of the membrane, cm
w_1	width of the flow channel, cm
x	distance perpendicular to membrane, cm
y_w	mole fraction of water in the flow channel
z	distance along flow channel, cm

Greek

δ_M	thickness of the catalyst-coated membrane, cm
λ	water content of the membrane
ρ_M	density of Nafion 1100, g/cm^3

References

1. T. E. Springer, T. A. Zawodzinski, and S. Gottesfeld, *J. Electrochem. Soc*., **138**, 2334 (1991).
2. D. M. Bernardi and M. Verbrugge, *AIChE J*., **37**, 1151 (1990).
3. T. V. Nguyen and R. E. White, *J. Electrochem. Soc*., **140**, 2178 (1993).
4. T. F. Fuller and J. Newman, *J. Electrochem. Soc*., **140**, 1218 (1993).
5. T. F. Fuller, Ph.D. Thesis, University of California, Berkeley, CA (1992).
6. J. S. Yi and T. V. Nguyen, *J. Electrochem. Soc*., **145**, 1149 (1998).
7. T. Okada, G. Kie, and M. Morton, *Electrochim. Acta*, **43**, 2141 (1998).
8. J. T. Hinatsu, M. Mizuhata, and H. Takenaka, *J. Electrochem. Soc*., **141**, 1493 (1994).
9. H. R. Zelsmann, M. Pineri, M. Thomas, and M. Escoubes, *J. Appl. Polym. Sci*., **41**, 1673 (1990).
10. T. A. Zawodzinski, T. E. Springer, J. Davey, R. Jestel, C. Lopez, J. Valerio, and S. Gottesfeld, *J. Electrochem. Soc*., **140**, 1981 (1993).
11. T. A. Zawodzinski, M. Neeman, L. O. Sillerud, and S. Gottesfeld, *J. Phys. Chem*., **95**, 6040 (1991).
12. T. A. Zawodzinski, C. Derouin, S. Radzinski, R. J. Sherman, V. T. Smith, T. E. Springer, and S. Gottesfeld, *J. Electrochem. Soc*., **140**, 1041 (1993).
13. K. Broka and P. Ekdunge, *J. Appl. Electrochem*., **27**, 117 (1997).
14. P. Schroeder, *Z. Phys. Chem*., **45**, 75 (1903).
15. S. W. Yeo and A. Eisenberg, *J. Appl. Polym. Sci*., **21**, 875 (1977).
16. W. Weppner and R. A. Huggins, *J. Electrochem. Soc*., **124**, 1569 (1977).